



RESEARCH MEMORANDUM

EFFECTS OF WING-MOUNTED TANK-TYPE STORES ON THE
LOW-LIFT BUFFETING AND DRAG OF A SWEEP-WING
AIRPLANE CONFIGURATION BETWEEN MACH
NUMBERS OF 0.8 AND 1.3

By Homer P. Mason

Langley Aeronautical Laboratory
Langley Field, Va.

*Mason Report Effective
2 RM-114 4-8-57
NA 4-20-57*

UNCLASSIFIED

CLASSIFIED DOCUMENT

This material contains information affecting the National Defense of the United States within the meaning of the espionage laws, Title 18, U.S.C., Secs. 793 and 794, the transmission or revelation of which in any manner to an unauthorized person is prohibited by law.

NATIONAL ADVISORY COMMITTEE FOR AERONAUTICS

WASHINGTON

October 6, 1955



NATIONAL ADVISORY COMMITTEE FOR AERONAUTICS

RESEARCH MEMORANDUM

EFFECTS OF WING-MOUNTED TANK-TYPE STORES ON THE
LOW-LIFT BUFFETING AND DRAG OF A SWEEP-WING
AIRPLANE CONFIGURATION BETWEEN MACH
NUMBERS OF 0.8 AND 1.3

By Homer P. Mason

SUMMARY

Two rocket-powered models of a 45° swept-wing airplane configuration have been tested with different underwing fuel-tank installations located at approximately half the wing semispan. Results of these tests have been compared with previously reported data from a similar configuration having no tanks and with isolated tank data. No severe low-lift buffeting was induced at transonic speeds by the addition to the airplane configuration of either of the two tank installations used in this investigation. One of the tanks used (designated tank A) was a parabolic body of revolution having a cambered (upswept) center line; the other tank (designated tank B) was a cylindrical body with an elliptical nose and had a volume comparable with that of tank A. The configuration with tank B had lower total drag coefficients at subsonic speeds than the configuration with tank A. Above a Mach number of 1.0, however, the installation with tank A was more favorable than the one with tank B. Approximately five times the isolated drag of tank B was added by its installation near a Mach number of 1.0 and about twice the isolated-tank drag was added at a Mach number of 1.2. Interference effects of tank B were approximately evenly divided between the effects of the tank installation on the wing-fuselage-pylon combination and the effects of the wing-fuselage-pylon combination on the tanks. Interference effects appeared to be generally the same with both tank installations although the isolated drag of tank A was not known. Both tank installations caused abrupt longitudinal trim changes at transonic speeds and a positive increment of lift at low angles of attack at supersonic speeds.



INTRODUCTION

Structural and operational limitations have been imposed on high-speed aircraft by the addition of external fuel, bomb, and missile storage. These limitations arise primarily from the mutual interference between the external store and the aircraft components and may result in large drag increments and poor buffet characteristics. A large amount of work (refs. 1 to 8, for example) has been done to evaluate these effects and to determine optimum store shapes and locations.

The present paper presents the results of flight tests of two rocket-powered research models having proposed tank-type stores beneath a 45° sweptback wing. One of the stores used (designated tank A) was a parabolic body of revolution having a cambered (upswept) center line; the other store (designated tank B) was a cylindrical body with an elliptical nose and had a volume comparable with that of tank A. These tests were conducted at the Langley Pilotless Aircraft Research Station at Wallops Island, Va.

SYMBOLS

α	angle of attack, deg
A	cross-sectional area, sq ft
a_l	longitudinal acceleration, g units
a_n	normal acceleration, g units
a_t	transverse acceleration, g units
b	wing span, ft
c	wing chord, ft
\bar{c}	mean aerodynamic chord, ft
C_D	drag coefficient, $\frac{\text{Drag}}{qS}$
C_L	lift coefficient, $\frac{\text{Lift}}{qS}$

C_m	pitching-moment coefficient, $\frac{\text{Moment}}{qS\bar{c}}$
C_Y	side-force coefficient, $\frac{\text{Side force}}{qS}$
$C_{L\alpha}$	lift-curve slope per degree, $\frac{\partial C_L}{\partial \alpha}$
$C_{m\alpha}$	slope of pitching-moment curve per degree, $\frac{\partial C_m}{\partial \alpha}$
F_S	net force on store in chordwise direction, lb
L	fuselage length, ft
M	Mach number
q	free-stream dynamic pressure, lb/sq ft
R	Reynolds number, based on \bar{c}
S	total wing area, sq ft

Subscripts:

n	forward accelerometer in fuselage
t	rearward accelerometer in fuselage
s	accelerometer in tank

MODELS

The airplane configuration used for these tests was the same as that of reference 1. This configuration had a parabolic fuselage of fineness ratio 10; 45° sweptback wings with aspect ratio of 3.56, taper ratio of 0.3, and NACA 64A007 airfoil sections parallel to the fuselage center line; and a cruciform-tail arrangement with 0° tail incidence. Principal dimensions of the model are shown in figure 1.

Two models were tested, each with two tank-type stores pylon-mounted at 0.494 wing semispan outboard from the fuselage center line with the tank plane of symmetry parallel to the fuselage center line. One model had stores which were approximately 0.12-scale models of the

North American Aviation, Inc., 275-gallon underwing tank for the North American F-100A airplane (hereinafter referred to as tank A). The other model had stores that were approximately 0.12-scale models of a tank shape developed by the Wright Air Development Center (ref. 8) (designated tank B) which were modified for these tests by increasing the length of the cylindrical section to obtain a volume comparable with that of tank A. The fineness ratio of the tank was thus changed from 7.75 to 8.83. Tank A was mounted on a cambered pylon - leading edge cambered toward the fuselage - which was also developed by North American Aviation, Inc., for use with tank A whereas tank B was mounted on a pylon similar to the Douglas 6-percent-thick 3-hook-shackle pylon (ref. 8). Details of the tanks and pylons are given in tables I to IV. Details of the installations are given in figures 2 to 4.

It should be noted here that the longitudinal location of tank A was not identical with its usual location on the full-scale airplane because of a design error in the model. Tanks were located with the tank center of gravity at 40 percent of the local wing chord rather than at the desired 40 percent of the mean aerodynamic chord. This error would correspond to moving the tank rearward approximately 17 inches on the full-scale airplane.

Photographs of the test models with the tanks installed are shown in figures 5 and 6, and one model-booster combination on the launcher is shown in figure 7. The longitudinal distribution of cross-sectional area with and without tanks is shown in figure 8.

INSTRUMENTATION

Both models tested had identical instrumentation as follows: a normal and a transverse accelerometer in the fuselage near the tail-root quarter chord; a normal, a transverse, and a longitudinal accelerometer in the fuselage near the wing-root quarter chord; a transverse accelerometer inside one tank near the pylon leading edge; a vane-type angle-of-attack indicator mounted on a sting ahead of the fuselage nose; and a beam-type balance in one tank to measure chordwise force between the tank and the pylon. A photograph of one tank with a side removed to show the chord-force balance and accelerometer installation is shown in figure 9.

All normal and transverse accelerometers had natural frequencies ranging from 97 to 123 cycles per second and had between 60 and 75 percent critical damping. These characteristics combined with recorder characteristics yielded system amplitude-response factors of the order of one at frequencies near the wing first-bending frequencies.

TESTS

Shake tests were conducted with each model to determine the approximate natural modes of vibration, and the natural frequencies are summarized as follows:

Model with -	Wing first bending, cps	Wing second bending, cps	Wing torsion, cps	Horizontal tail first bending, cps
No tanks	62	210	300	126
Tank A	56	191	200	138
Tank B	60	195	246	136

Other frequencies were observed which appeared to be combinations of wing bending and torsion with probably some distortion due to the pylon and tank installations. These vibrations occurred at frequencies near the wing second-bending frequency and were most evident on the model with tank A.

Flight tests were conducted by using external booster rocket motors to accelerate the models to a Mach number of approximately 1.4, after which the model separated from the booster and coasted through the test Mach number range. Data presented herein were obtained by standard NACA telemetering of model information during coasting flight. Velocity data were obtained from the CW Doppler radar set, flight-path data were obtained from SCR 584 tracking radar, and rolling velocity was obtained from a spinsonde recorder and the model telemeter antenna. Atmospheric data were obtained from a radiosonde released between the test flights which were about one and one-half hours apart. Dynamic pressure and Reynolds number based on the wing mean aerodynamic chord of 1.345 feet are presented in figure 10. Atmospheric temperature and pressure data are shown in figure 11. The wing loading of both models of these tests was approximately 25 pounds per square foot.

ACCURACY

The maximum errors which may be present in the data of these tests, as estimated from considerations of instrument accuracies and the scatter of data points, are summarized in the following table:

α , deg	± 0.5
C_L	± 0.02
C_Y	± 0.02
C_D , total	± 0.002
C_D , for two tanks	± 0.001
M	± 0.02

The above values are for Mach numbers near 0.9, and may be reduced by approximately 50 percent at Mach numbers near 1.2. These values apply to the basic data points through which the curves presented herein were faired. It is believed that the accuracy of the faired curves is appreciably better than the above values indicate.

RESULTS AND DISCUSSION

Results of flight tests of two models each of which had two tank-type stores mounted on pylons beneath a 45° sweptback wing are presented herein and are compared with data from a similar model having no tanks (ref. 1).

Trim

Trim characteristics of both models having external tanks and the reference model having no stores are plotted against Mach number in figure 12. It may be seen that the external tanks induced a positive lift coefficient at small angles of attack throughout the supersonic Mach number range of the tests and caused an abrupt trim change at transonic speed. The external tanks had little or no effect on the trim side-force coefficients.

Buffeting

Portions of the telemeter records obtained in the present investigation are reproduced in figure 13. It is immediately obvious from the normal- and transverse-accelerometer traces that some small-amplitude oscillatory or vibratory phenomenon was experienced by these models. The oscillations, or roughness, evident on the records obtained from the model with tank B were milder than those on the records from the model with tank A. The principal frequencies at which model response is evident in these records correspond in each case to the model pitching and yawing frequency with wing first bending and some other higher order structural frequencies superimposed.

As may be seen in figure 13, the observed roughness did not occur continuously throughout the test Mach number range. Rather, the observed oscillatory accelerations occurred in bursts with the larger amplitudes below about $M = 0.9$, some very small amplitudes near $M = 1.2$ (not shown), and with practically no indication of roughness, except for a trim change, between Mach numbers of about 0.9 and 1.0. Thus, the observed roughness does not appear to be consistent with penetration of the low-lift buffet boundary.

The telemeter records of the present tests are very similar in appearance to the records obtained from the model of reference 1. This model, however, experienced its only roughness near $M = 1.2$, and again there is no consistency with penetration of the low-lift buffet boundary.

A possible explanation of the roughness observed in the present tests may be found from a comparison of the telemeter records of these tests with those of reference 9. The models of reference 9 were flight tested on days during which the air along the model flight path was known to be turbulent. It may be seen in reference 9 that one of the primary effects of turbulence on a model is an excitation of the model pitching and yawing natural frequencies in an unsteady manner and that higher structural frequencies are superimposed on the pitch and yaw response. Such excitation is evident in the response of the models of the present tests and of the model of reference 1. Consultation with the meteorologists of the Langley Flight Research Division revealed that the present tests were conducted in air that was probably moderately turbulent. A study of atmospheric data from the test of the model of reference 1 indicated that turbulence was likely at about the altitude where roughness was indicated by the model accelerations. Thus, it appears that a large part of the roughness encountered in the present tests and in the test of reference 1 was probably the result of atmospheric turbulence along the model flight path.

Consultation with the meteorologists further revealed that atmospheric data such as shown in figure 11 may provide an indication of the existence of atmospheric turbulence. It is believed that comparison of the actual lapse rate (the rate of change of temperature with pressure altitude) with that for wet or dry adiabatic expansion provides such indication in most cases. However, the lapse-rate comparison is not necessarily a sufficient criterion and, as in the present tests, additional factors such as relative humidity and wind direction and velocity must be considered.

It cannot be stated, however, that all the roughness evident in the subject records was due to turbulence. Accelerations similar in appearance to those of the present tests have been observed on comparable models in atmospheric conditions such that turbulence would not be expected (refs. 1 and 2). This roughness is considered to be buffeting. Further,

unpublished data lead to the idea that turbulence in the air may actually induce buffeting, or a similar phenomenon, of a configuration flying near its buffet boundary.

In the light of the previous discussion, it cannot be stated conclusively that buffeting was or was not experienced by either of the test configurations; thus, no conclusion relative to the effects of tank shape on configuration buffeting can be stated. Since buffeting results primarily in excitation of structural frequencies and since the structural vibrations observed in the present tests were consistently small, it may be concluded that addition of either of the widely different tank installations of the present tests to the basic wing-fuselage combination did not induce any severe buffeting of the test configurations.

Drag

Total-drag coefficients, based on the wing total area, are compared in figure 14 with the drag coefficient of the model of reference 1 with no stores. Addition of either of the tank assemblies of the present tests to the basic airplane configuration resulted in a slightly lowered drag-rise Mach number and much higher total drag. The configuration with tank B had lower total drag than the configuration with tank A below about $M = 0.99$; however, above $M = 0.99$ the model with tank A appears to have the lower total drag.

The normal cross-sectional area distributions of the models tested are presented in figure 8 so that the drag rises of the configurations could be compared according to the concept of the transonic area rule. Although the area distributions of the models with stores are approximately the same, the drag rise of the configuration with tank B was about 14 percent higher than that for the configuration with tank A at Mach number of 1.0.

Total installation drag coefficients of each tank installation are shown in figure 15 and are compared with the measured tank drag coefficients in the presence of the wing-fuselage combination. Drag coefficients of the isolated tank B from reference 5 are also shown for comparison. These data are believed to be comparable since the only modification was an increase in the length of the cylindrical center section which should have a negligible effect on the isolated drag coefficient. Both isolated drag coefficients and drag coefficients of the tanks in the presence of the fuselage, wing, and pylon were measured on only one tank and were doubled in figure 15 for ease of comparison. Estimated drag coefficients of the pylons of the present tests are small compared with the other drag increments. Thus it may be concluded that nearly all the installation drag above the level of the isolated tank drag was caused by interference.

Approximately 45 percent of the total installation drag of tank B near $M = 1.0$ is directly traceable to the interference of the tanks on the wing-fuselage configuration. This effect decreased to about 25 percent of the installation drag near $M = 1.2$. About 35 percent of the total installation drag of tank B near $M = 1.0$ is traceable to the interference of the wing-fuselage combination on the tanks. This effect also decreases to about 25 percent of the installation drag near $M = 1.2$. Thus, about 80 percent of the total installation drag, or 4 times the isolated tank drag, caused by tank B near $M = 1.0$ was the result of interference; and about 50 percent of the total installation drag, or the same order as the isolated tank drag, was caused by interference near $M = 1.2$. These data do not indicate any further appreciable decrease of the interference drag with increasing Mach number within the test limits. These data are in qualitative agreement with the data of reference 7 in that the total interference drag at supersonic speeds appears about evenly divided between the effect of the wing-fuselage-pylon combination on the tanks and the effects of the tanks on the wing-fuselage-pylon combination.

Although isolated tank drag data for tank A are not available, the data of these tests are generally consistent with the data for tank B in regard to the interference increments at transonic speeds. The total installation drag of tank A, however, continued to decrease with increasing Mach number at supersonic speeds whereas the installation drag of tank B appears to level off near $M = 1.2$ and remain at a slightly higher level than for tank A.

Static Longitudinal Stability

The variations of lift coefficient and pitching-moment coefficient with angle of attack at small angles of attack are shown in figure 16 for both models at $M = 1.26$. Pitching moments were measured about the model center of gravity which was located at approximately 27.5 percent mean aerodynamic chord. These data were obtained from free oscillations of the model which resulted from booster separation and show no nonlinearities within the angle-of-attack range and scatter of data of these tests. Both configurations had positive pitching moments at zero lift and positive lift at zero angle of attack, which is in qualitative agreement with data of references 6 and 7. These data indicate that the center of pressure of both configurations was at approximately 69.5 percent of the mean aerodynamic chord at $M = 1.26$. No effect of tank shape on the static longitudinal stability of the configuration is apparent in the data of these tests.

CONCLUSIONS

Two rocket-powered models of a 45° swept-wing airplane configuration have been tested with different underwing fuel-tank installations. One of the tanks (designated tank A) was a parabolic body of revolution having a cambered (upswept) center line; the other tank (designated tank B) was a cylindrical body with an elliptical nose and had a volume comparable with that of tank A. Results of these tests have been compared with previously reported data from a similar configuration without tanks and with isolated-tank data. The following conclusions are indicated:

1. No severe low-lift buffeting was induced at transonic speeds by the addition of either of the two tank installations used in this investigation.
2. The configuration with tank B had lower total drag coefficients than the configuration with tank A at subsonic speeds. Above a Mach number of about 1.0, the total drag of the configuration with tank A was more favorable than that of the configuration with tank B.
3. The drag added by tank B amounted to about five times the isolated tank drag at a Mach number of 1.0 and about twice the isolated tank drag at a Mach number of 1.2. The interference effects appear to be about evenly divided between the effects of the tank on the wing-fuselage-pylon combination and the effects of the wing-fuselage-pylon combination on the tank.
4. Both of the tank installations tested caused an abrupt longitudinal trim change at transonic speeds and a positive increment of lift at low angles of attack at supersonic speeds.

Langley Aeronautical Laboratory,
National Advisory Committee for Aeronautics,
Langley Field, Va., April 5, 1955.

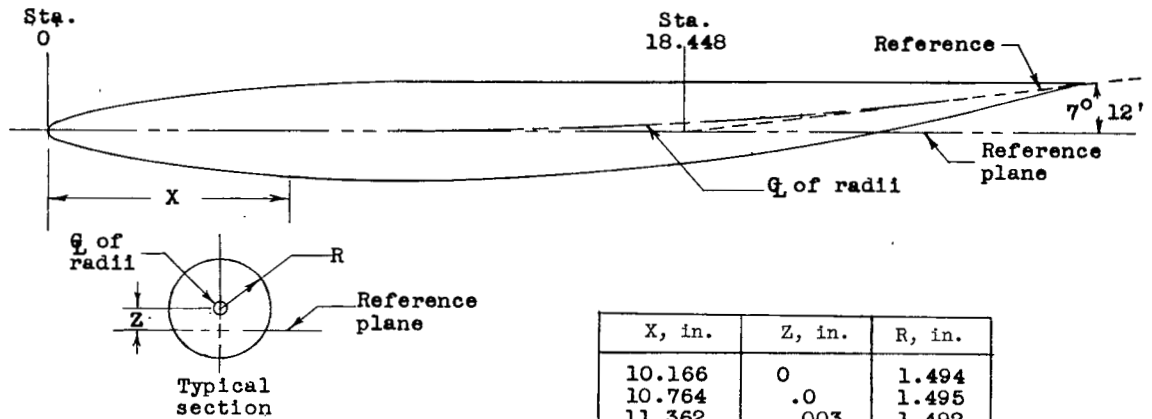
REFERENCES

1. Mason, Homer P.: Flight Test Results of Rocket-Propelled Buffet-Research Models Having 45° Sweptback Wings and 45° Sweptback Tails Located in the Wing Chord Plane. NACA RM L53I10, 1953.
2. Henning, Allen B.: The Effects of Wing-Mounted External Stores on the Trim, Buffet, and Drag Characteristics of a Rocket-Propelled Model Having a 45° Sweptback Wing. NACA RM L54B19, 1954.
3. Hoffman, Sherwood, and Wolff, Austin L.: Effect on Drag of Longitudinal Positioning of Half-Submerged and Pylon-Mounted Douglas Aircraft Stores on a Fuselage With and Without Cavities Between Mach Numbers 0.9 and 1.8. NACA RM L54E26, 1954.
4. Alford, William J., Jr., and Silvers, H. Norman: Investigation at High Subsonic Speeds of Finned and Unfinned Bodies Mounted at Various Locations From the Wings of Unswept- and Swept-Wing—Fuselage Models, Including Measurements of Body Loads. NACA RM L54B18, 1954.
5. Mason, Homer P., and Henning, Allen B.: Effects of Some External-Store Mounting Arrangements and Store Shapes on the Buffet and Drag Characteristics of Wingless Rocket-Powered Models at Mach Numbers From 0.7 to 1.4. NACA RM L54I20a, 1954.
6. Jacobsen, Carl R.: Effects of the Spanwise, Chordwise, and Vertical Location of an External Store on the Aerodynamic Characteristics of a 45° Sweptback Tapered Wing of Aspect Ratio 4 at Mach Numbers of 1.41, 1.62, and 1.96. NACA RM L52J27, 1953.
7. Smith, Norman F., and Carlson, Harry W.: The Origin and Distribution of Supersonic Store Interference From Measurement of Individual Forces on Several Wing-Fuselage-Store Configurations. I.—Swept-Wing Heavy-Bomber Configuration With Large Store (Nacelle). Lift and Drag; Mach Number 1.61. NACA RM L55A13a, 1955.
8. Dugan, James C.: External Store Development. Memo. Rep. No. WCNSR-43019-1-1, Wright Air Dev. Center, U. S. Air Force, Aug. 31, 1951.
9. Vitale, A. James: Characteristics of Loads in Rough Air at Transonic Speeds of Rocket-Powered Models of a Canard and a Conventional-Tail Configuration. NACA RM L54L17, 1955.

TABLE I

BASIC LINES AND COORDINATES OF TANK A

[Contour to the rear of station 26.312 is faired into a cone with its vertex at station 30.218 and its axis parallel to the 7° 12' reference]

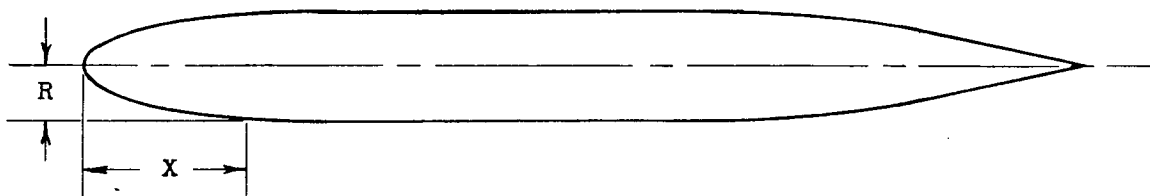


X, in.	R, in.
0	0
.598	.412
1.196	.583
1.794	.714
2.392	.824
2.990	.921
3.588	1.010
4.186	1.090
4.784	1.164
5.382	1.230
5.980	1.289
6.578	1.340
7.176	1.384
7.774	1.421
8.372	1.450
8.970	1.472
9.568	1.487

X, in.	Z, in.	R, in.
10.166	0	1.494
10.764	.0	1.495
11.362	.003	1.492
11.960	.009	1.486
12.558	.017	1.478
13.156	.029	1.466
13.754	.043	1.452
14.352	.060	1.435
14.950	.080	1.415
15.548	.102	1.393
16.146	.128	1.367
16.744	.156	1.340
17.342	.187	1.308
17.940	.221	1.274
18.538	.258	1.237
19.136	.298	1.197
19.734	.340	1.155
20.332	.385	1.110
20.930	.433	1.062
21.528	.484	1.011
22.126	.538	.957
22.724	.595	.900
23.322	.654	.840
23.920	.717	.778
24.518	.782	.713
25.116	.850	.645
25.714	.920	.575
26.312	.994	.501
30.218	1.495	0

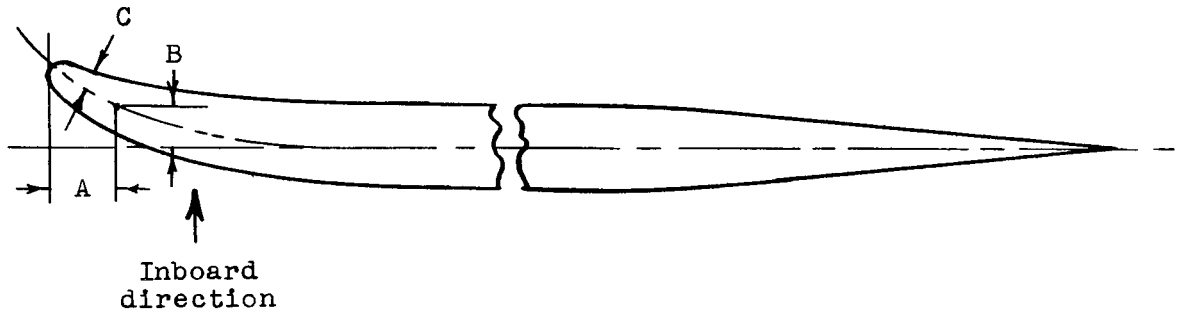
TABLE II
 COORDINATES OF TANK B

[Contour to the rear of station 19.648 is a cone
 with vertex at station 24.312]



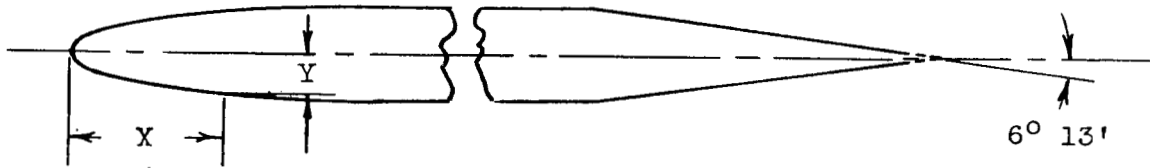
X, in.	R, in.
0	0
.120	.285
.239	.401
.478	.561
.718	.679
1.316	.893
1.914	1.043
2.512	1.154
3.110	1.239
3.708	1.300
4.306	1.343
4.904	1.367
5.502	1.375
16.060	1.375
16.658	1.367
17.256	1.343
17.854	1.300
18.452	1.239
19.050	1.154
19.648	1.043
24.312	0.0

TABLE III
COORDINATES OF PYLON USED WITH TANK A

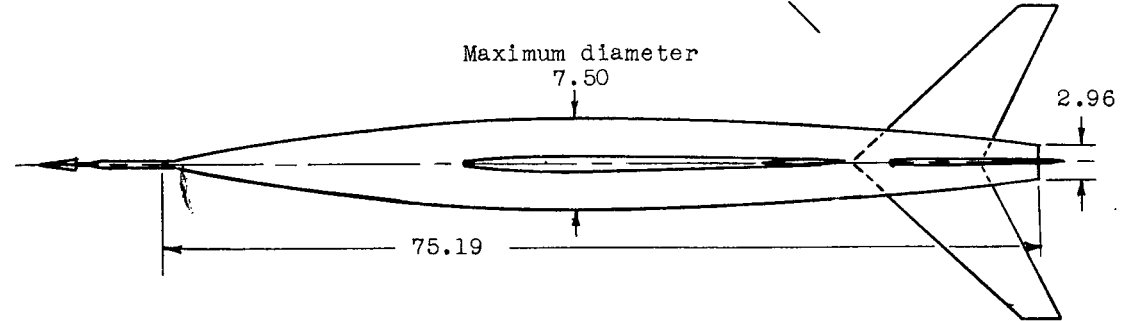
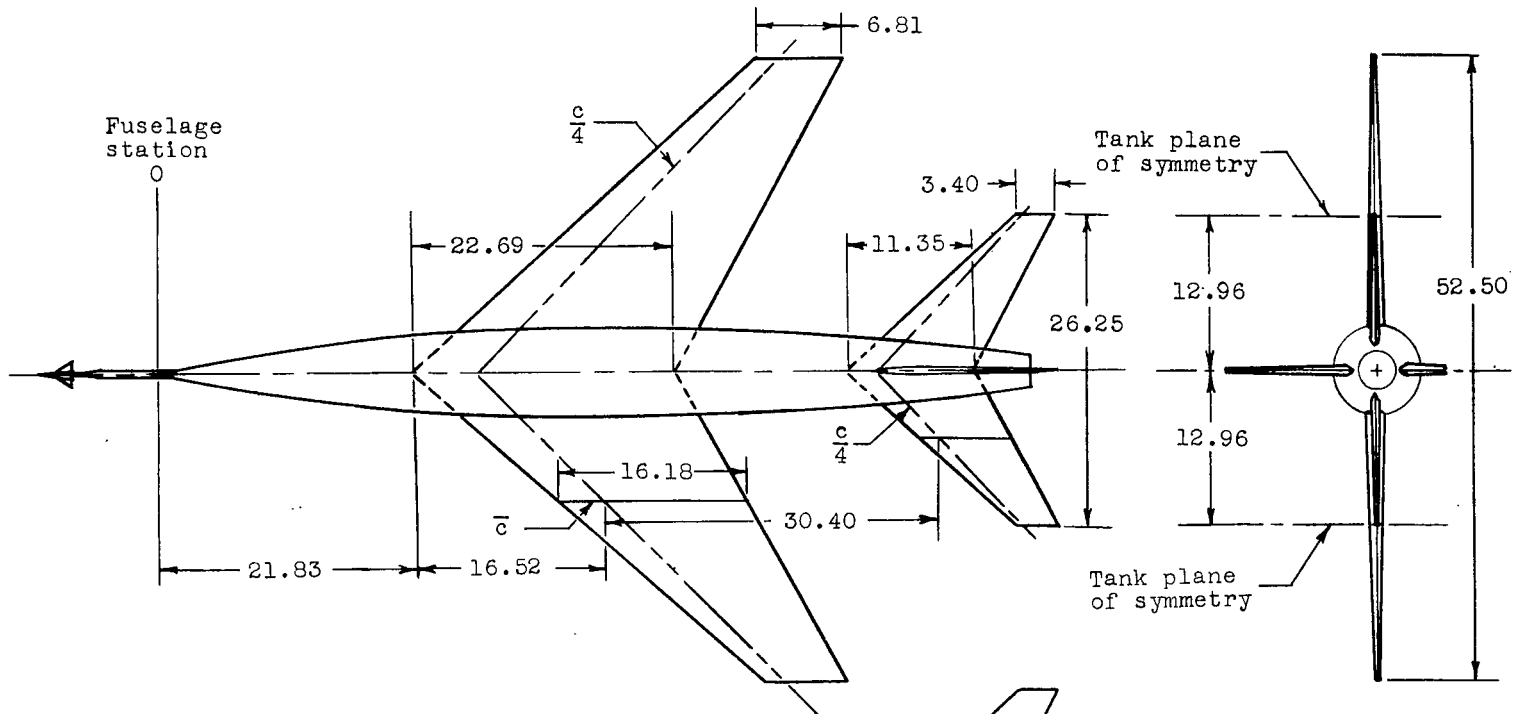


A, in.	B, in.	C, in.
0	0.239	0
.025		.029
.030	.226	—
.042	—	.038
.060	.217	—
.120	.198	—
.169	—	.070
.239	.161	—
.254	—	.084
.478	.097	—
.507	—	.114
.718	.050	—
.846	—	.138
.957	.021	—
1.184	—	.148
1.353	0	.150
7.658	—	.150
7.827	—	.146
7.996	—	.140
8.335	—	.120
8.673	—	.094
9.011	—	.063
9.349	—	.032
9.688	—	0
Constant section between pylon station 1.353 and 7.658		

TABLE IV
 COORDINATES OF PYLON USED WITH TANK B
 [Douglas 3-hook-shackle pylon]

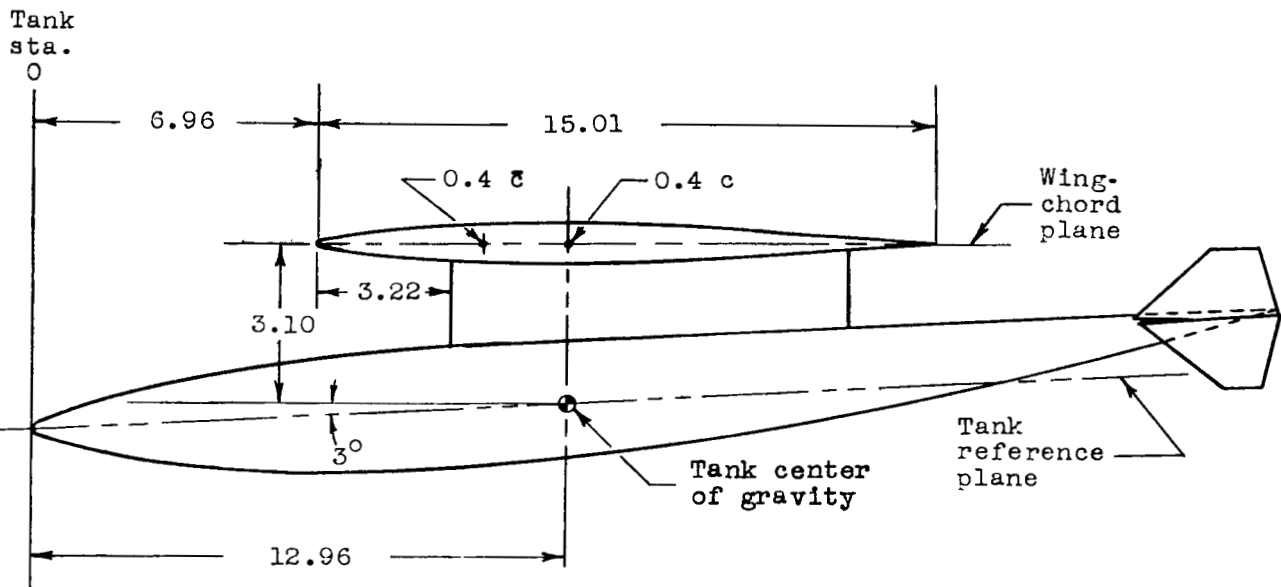


X, in.	Y, in.
0	0
.060	.070
.120	.098
.179	.119
.239	.136
.299	.150
.598	.202
.897	.234
1.196	.254
1.495	.265
1.722	.267
6.458	.267
8.910	0
Leading-edge radius	0.064
Trailing-edge radius	0.038
Actual chord length	8.611
Constant section between pylon station 1.722 and 6.458	

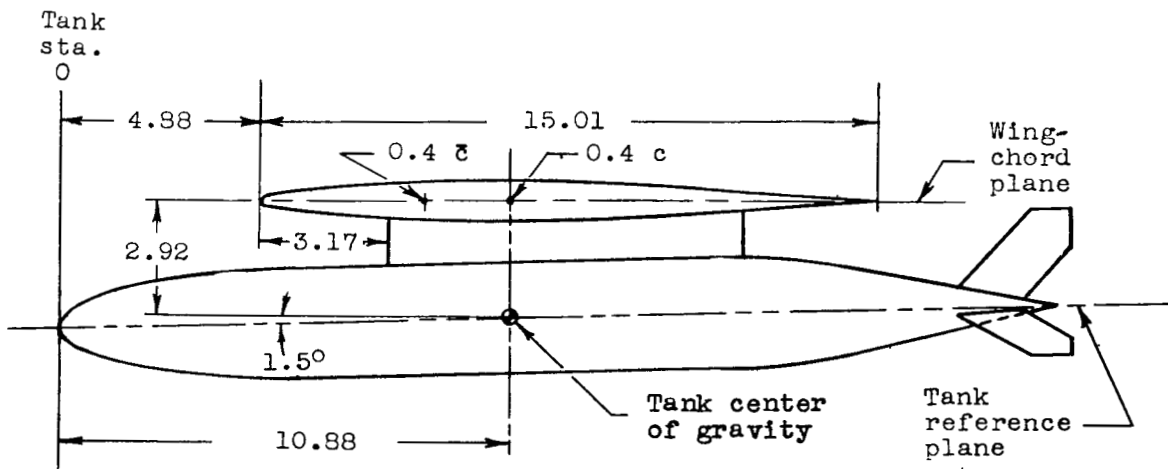


- All surfaces
- Aspect ratio 3.56
- Taper ratio 0.3
- Sweepback, $0.25c$ 45°
- Airfoil section,
streamwise NACA 64A007
- Wing area, total, sq ft 5.38
- Tail area, total each
plane, sq ft 1.35

Figure 1.- Principal dimensions and geometric characteristics of test models. All dimensions are in inches.



Tank A



Tank B

Figure 2.- Installation details of tank assemblies. All dimensions are in inches. Tank plane of symmetry and pylon reference plane are coincident and parallel to the fuselage center line at the 0.494b/2 wing station.

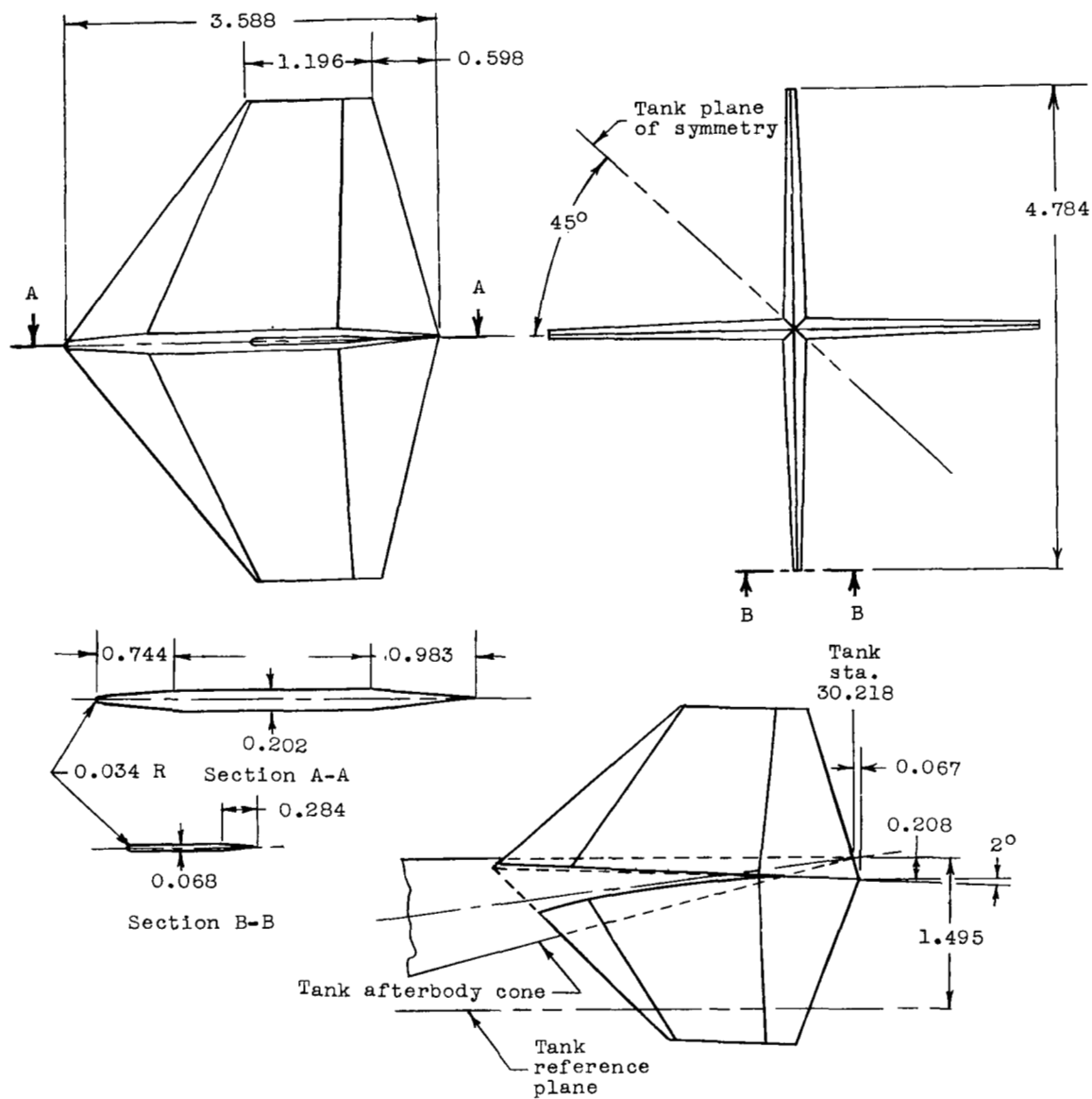


Figure 3.- Stabilizing fins of tank A. All dimensions are in inches.

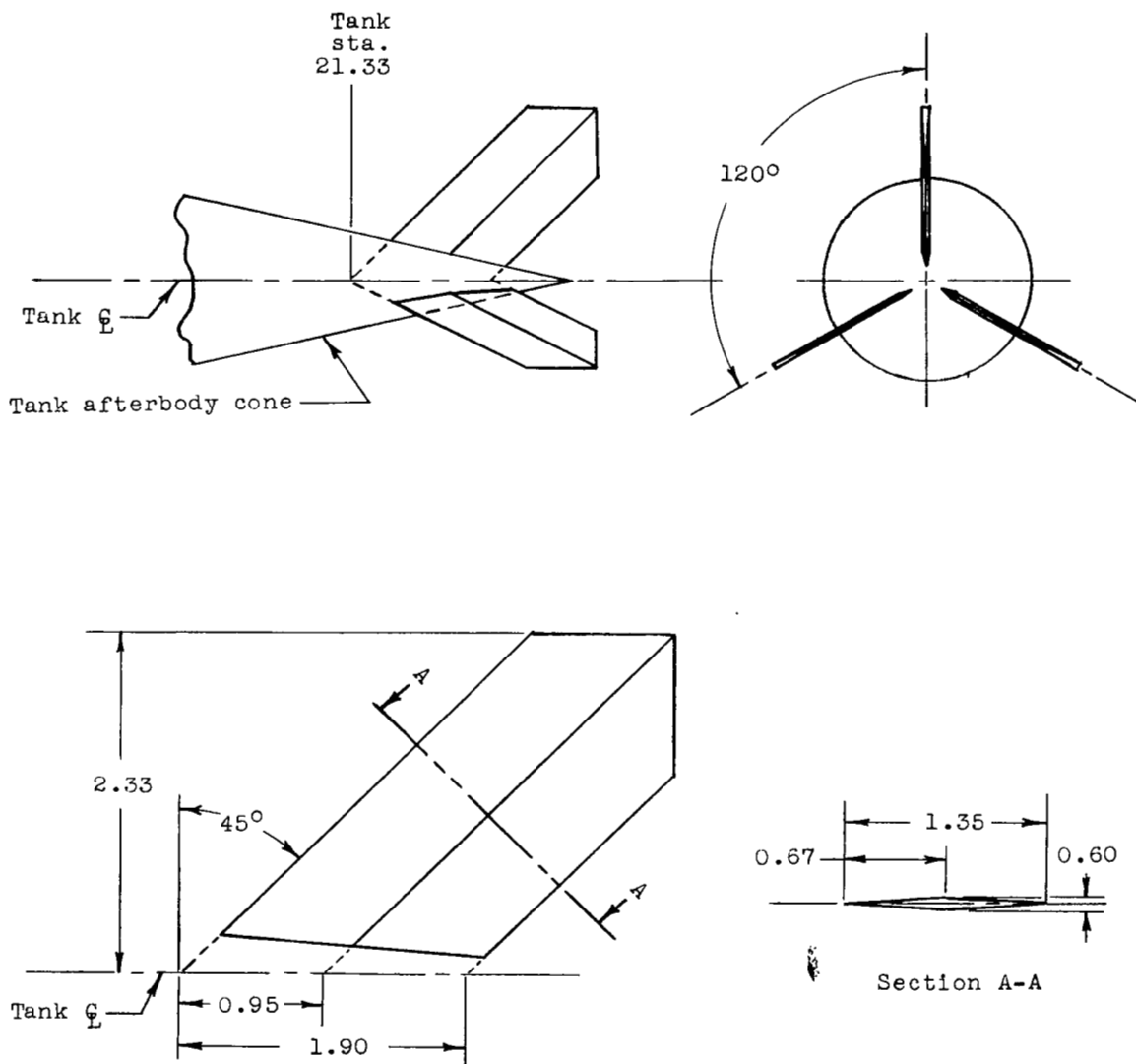
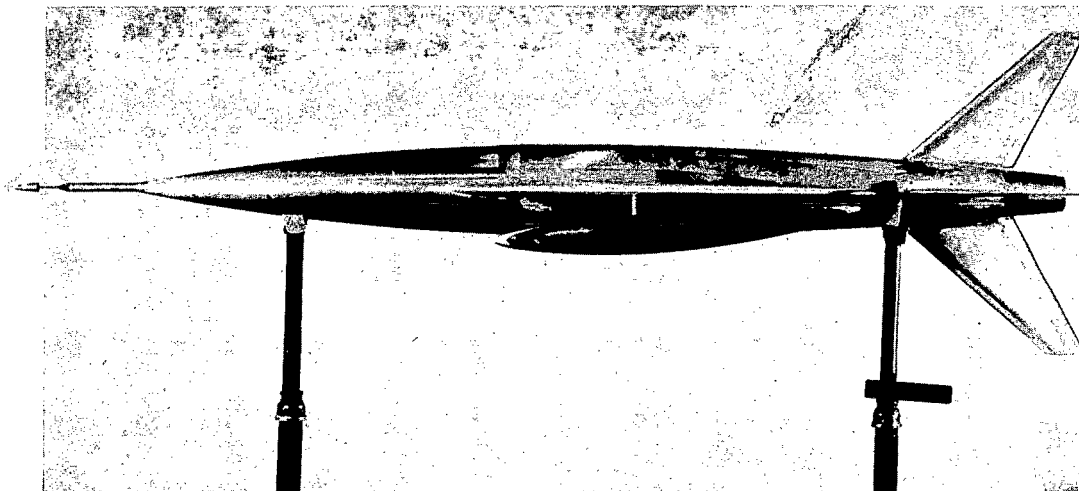


Figure 4.- Stabilizing fins of tank B. All dimensions are in inches.



L-84752.1

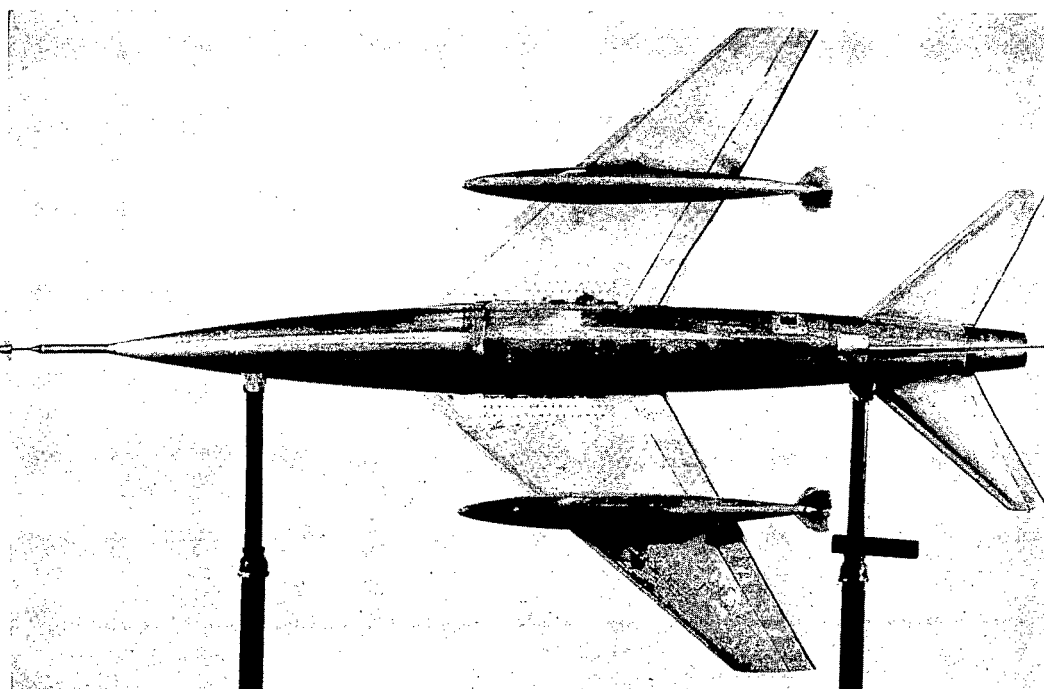
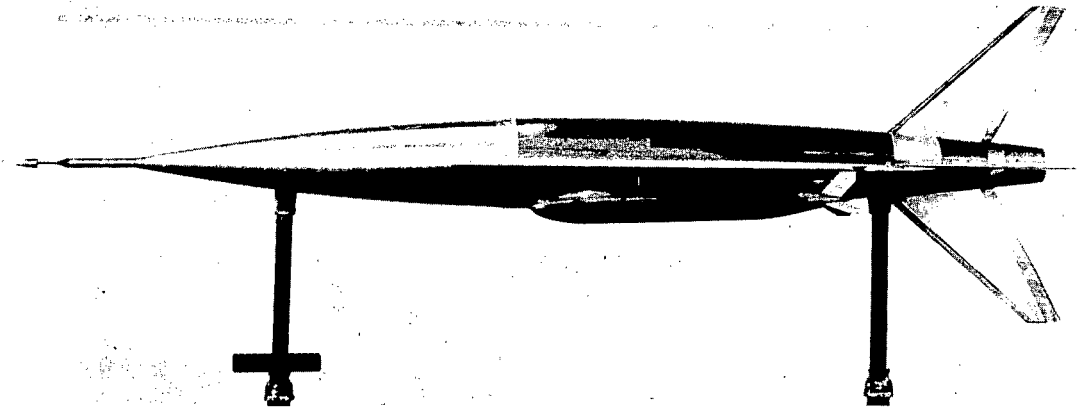


Figure 5.- Photographs of model with tank A.

L-84751.1



L-84741.1

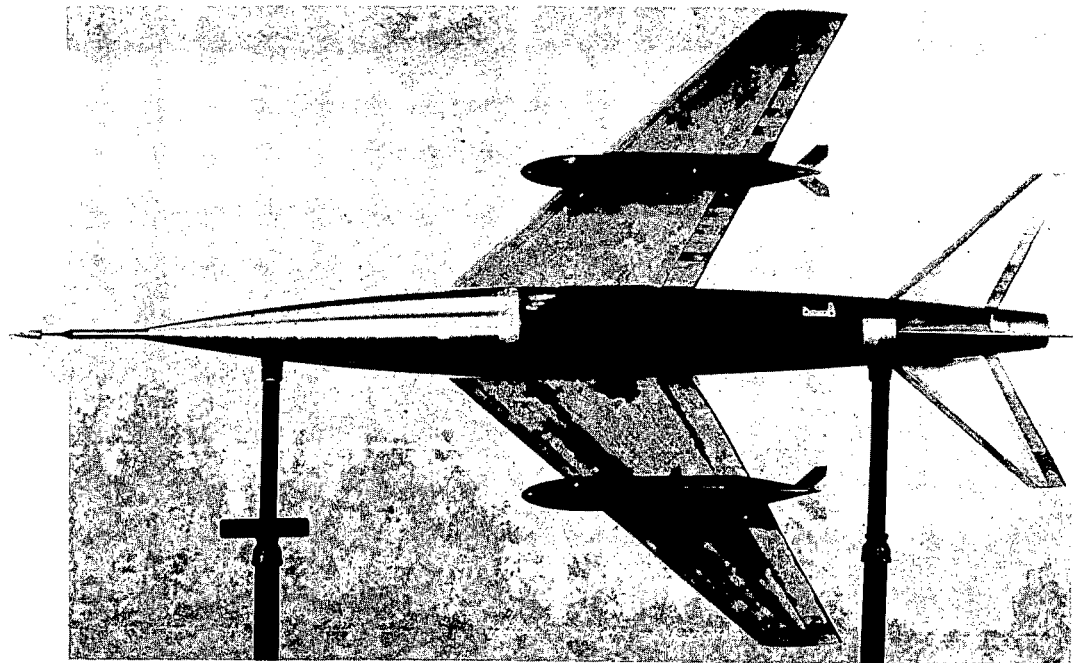
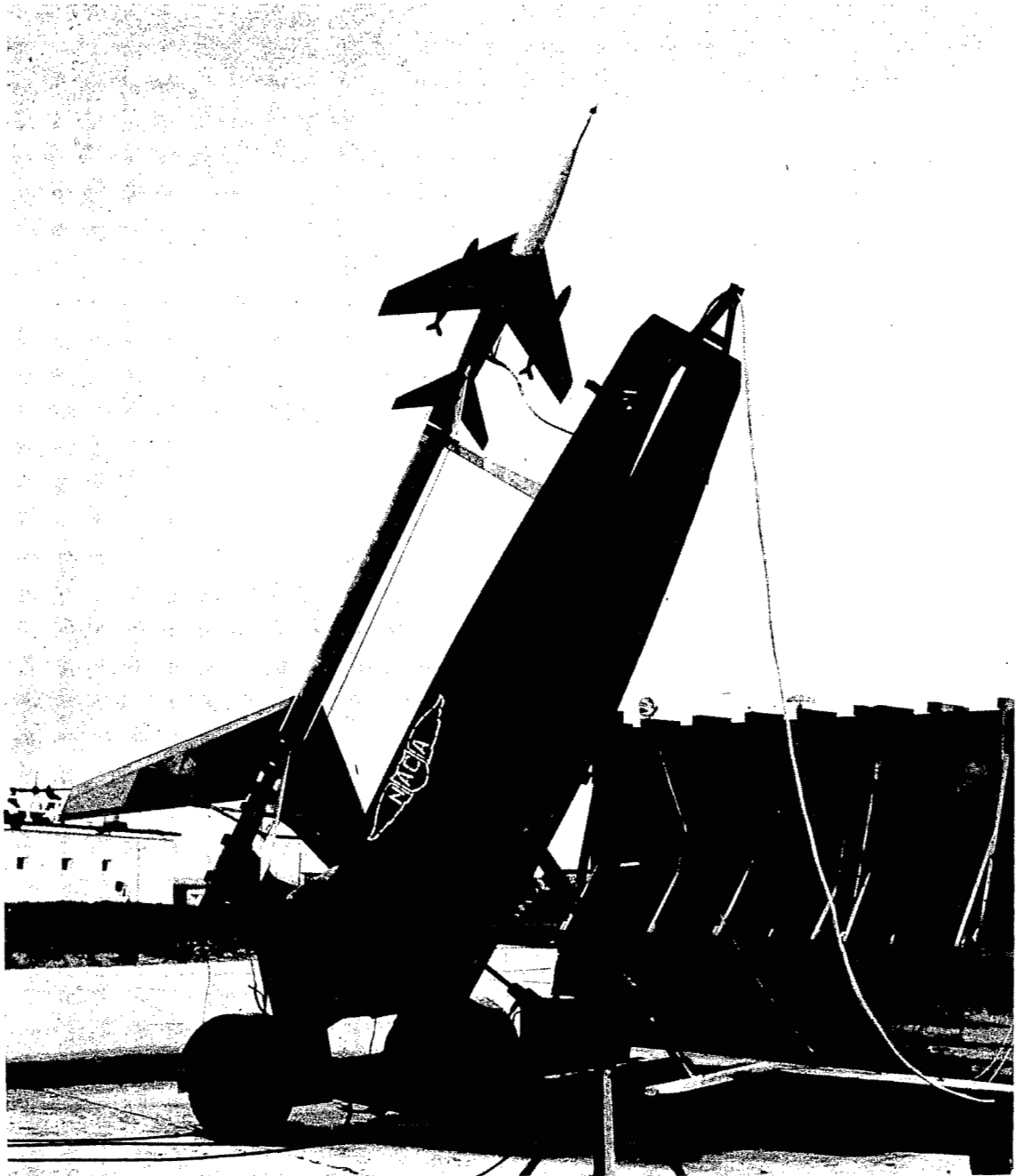


Figure 6.- Photographs of model with tank B.

L-84742.1



L-85045

Figure 7.- Photograph of a model-booster combination on the launcher.

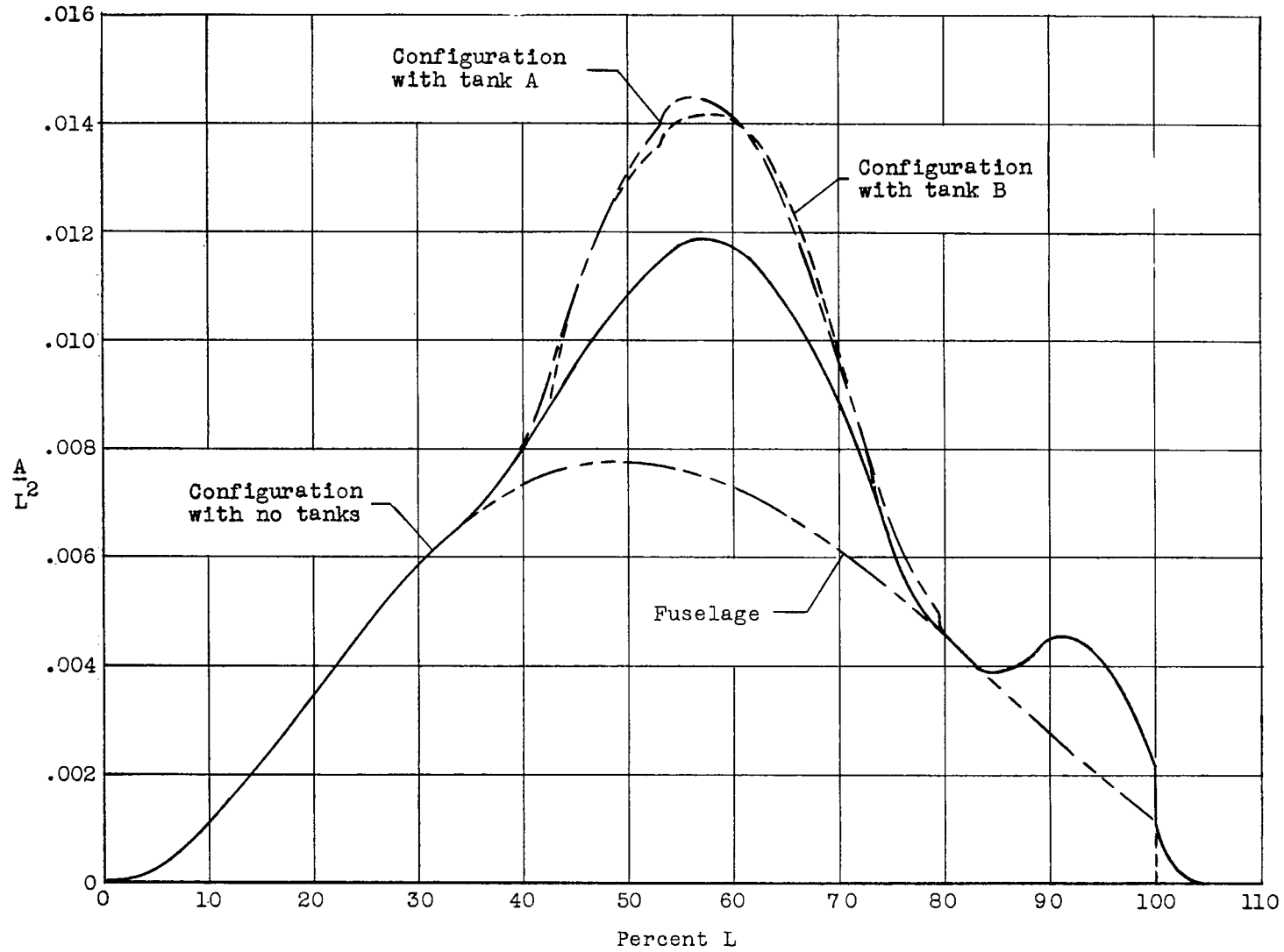
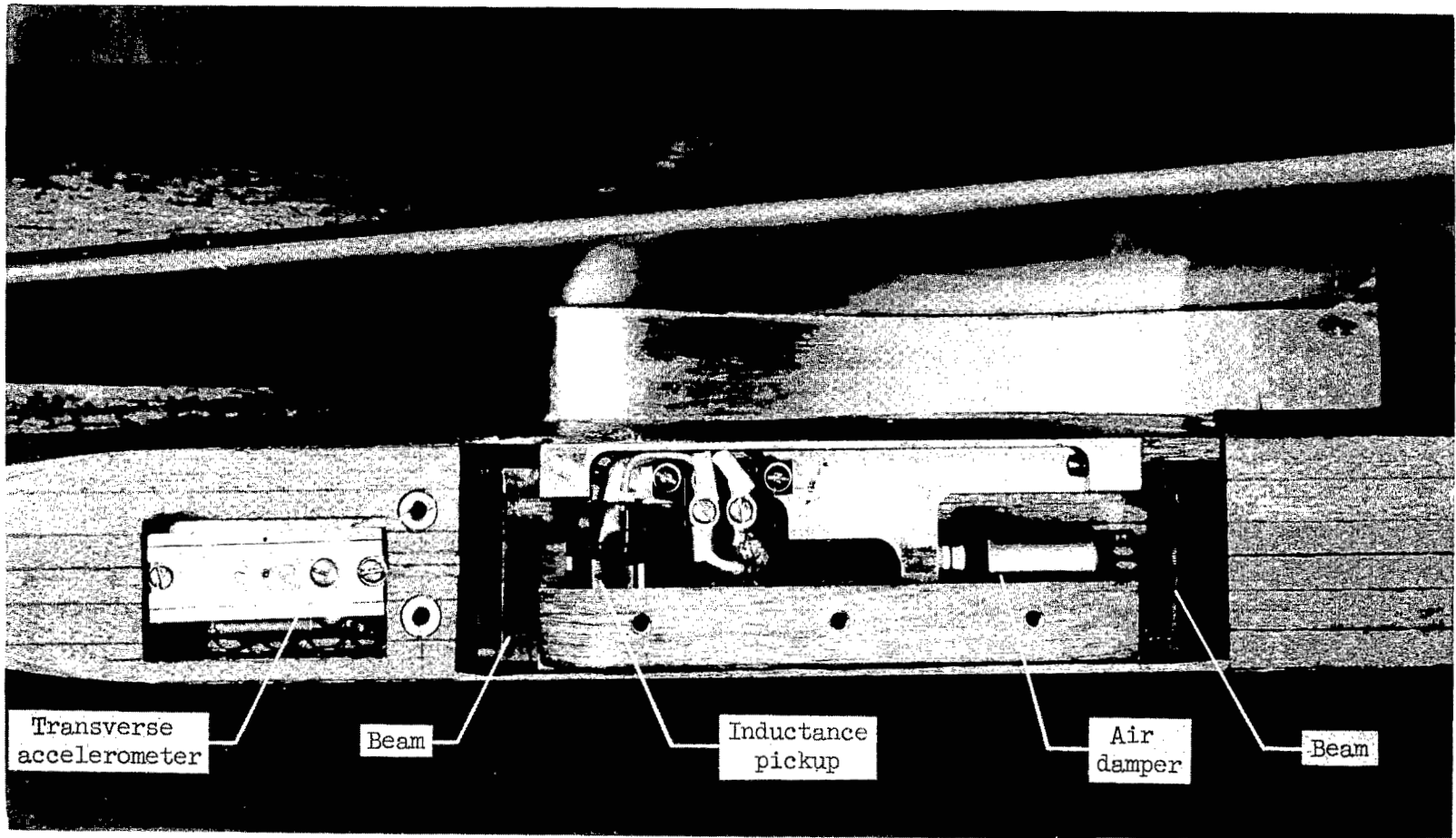


Figure 8.- Longitudinal distribution of cross-sectional area.



Transverse
accelerometer

Beam

Inductance
pickup

Air
damper

Beam

L-84740.1

Figure 9.- Photograph of balance used to measure drag of one store in the presence of pylon and wing.

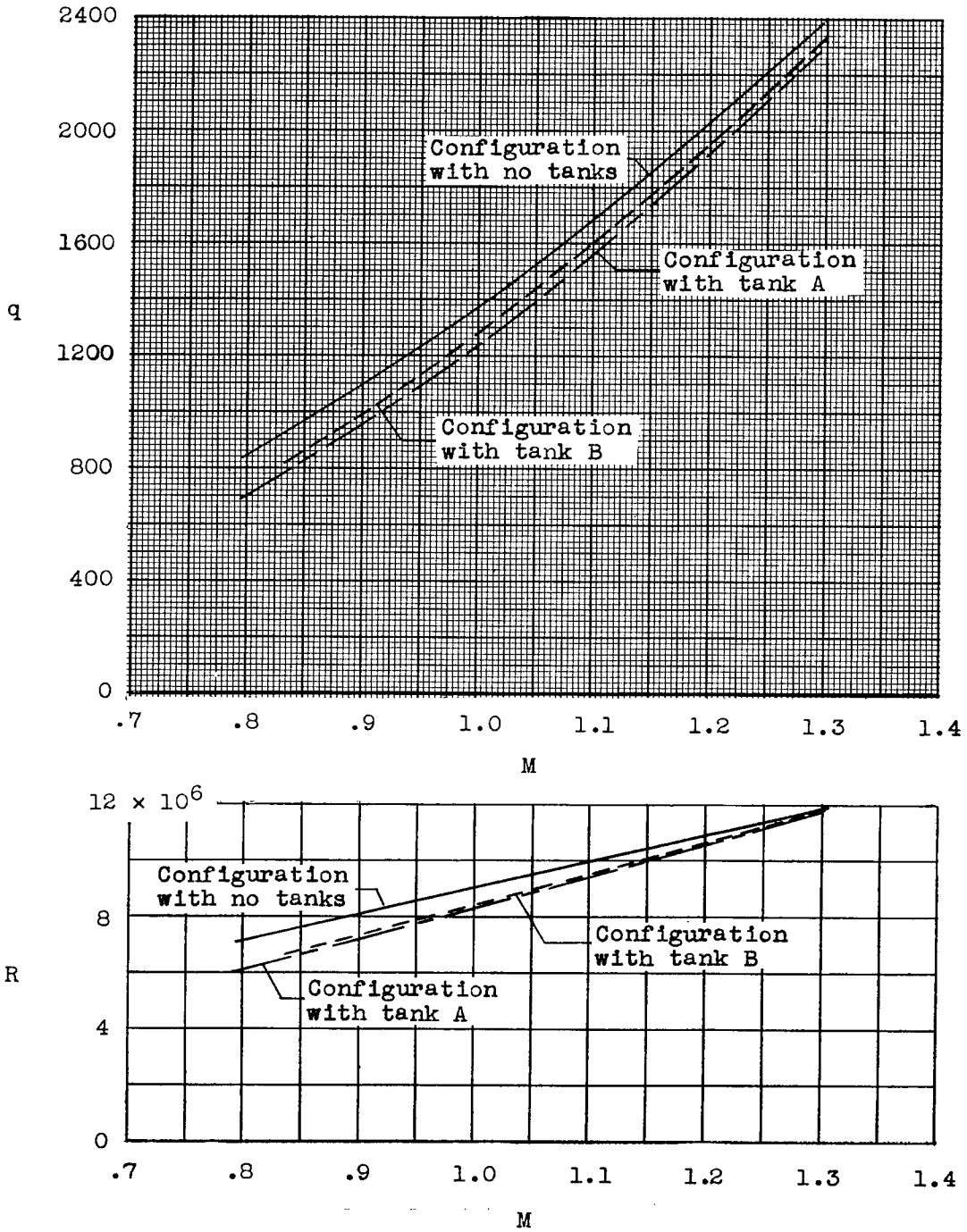


Figure 10.- Variation of dynamic pressure and Reynolds number with Mach number.

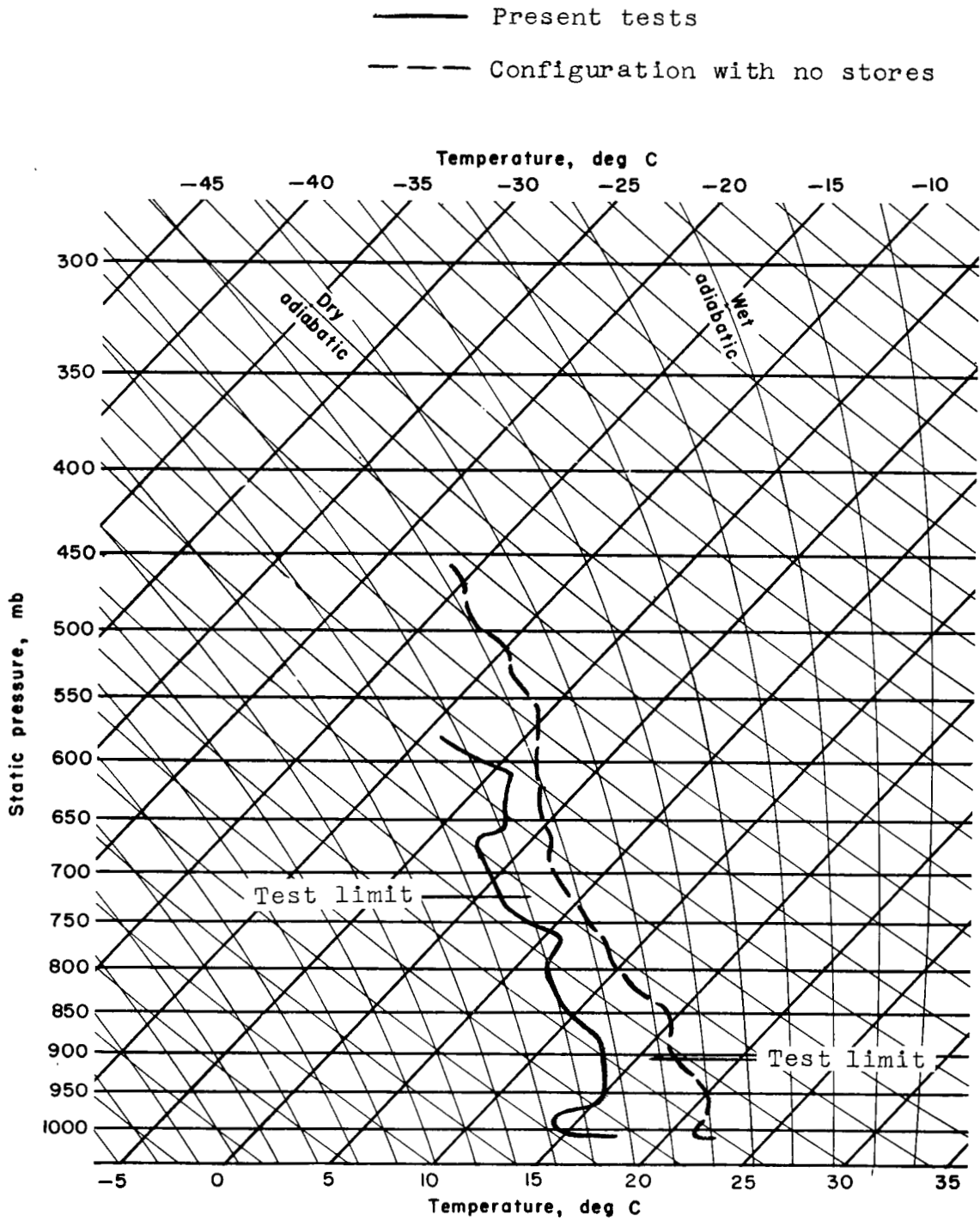


Figure 11.- Reproduction of a portion of a USAF skew T, log p diagram with atmospheric data from the present and reference tests.

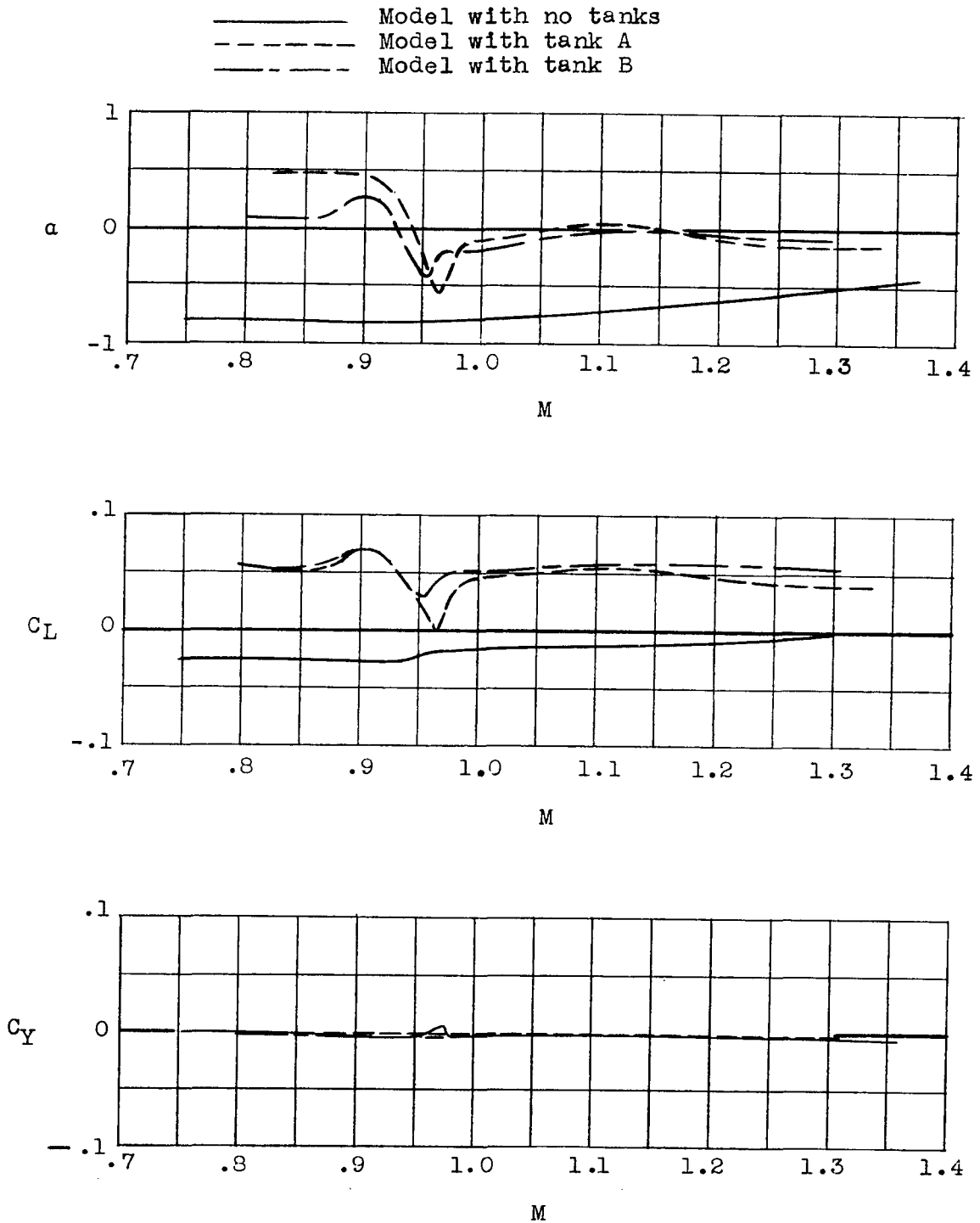
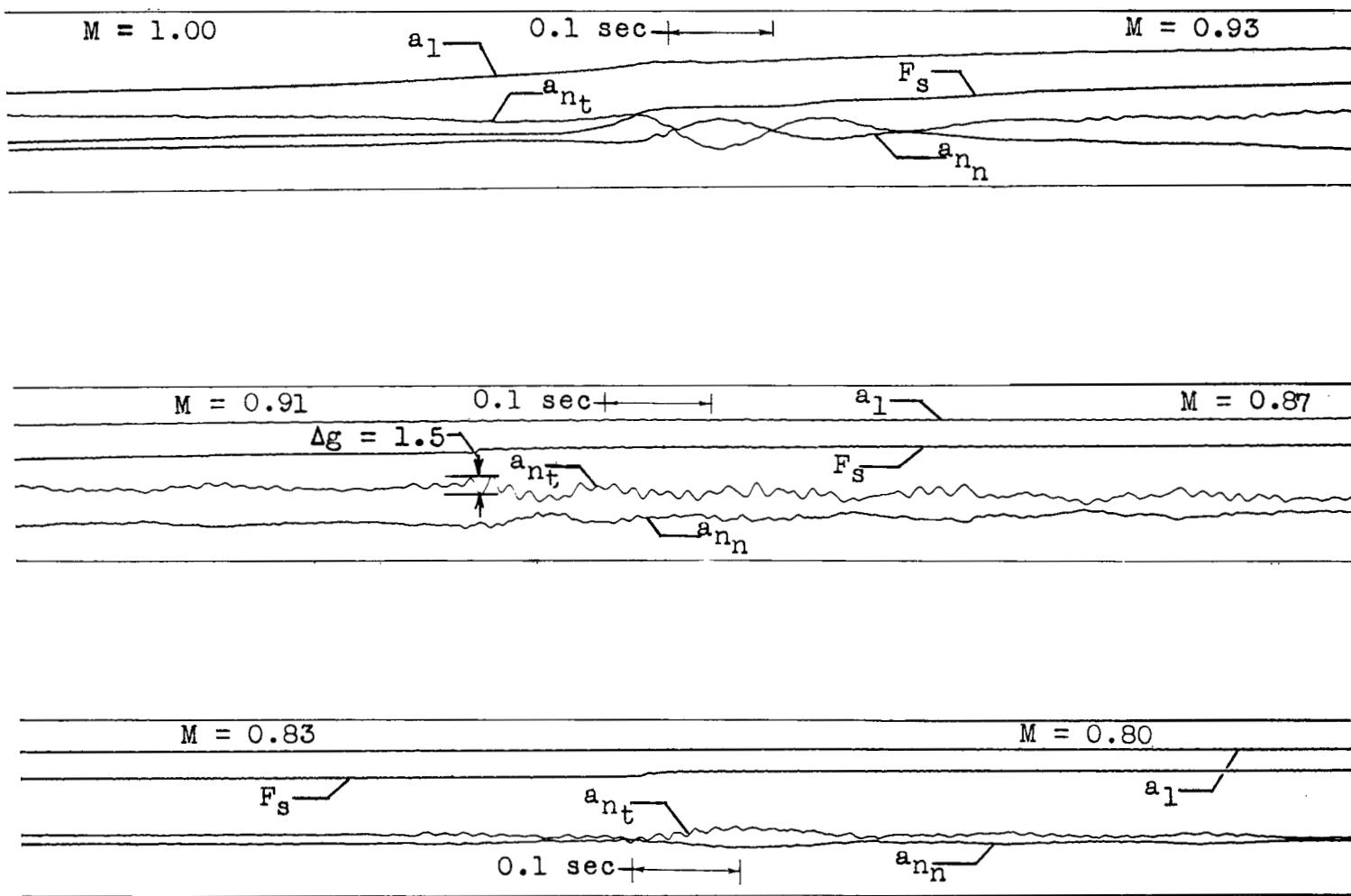
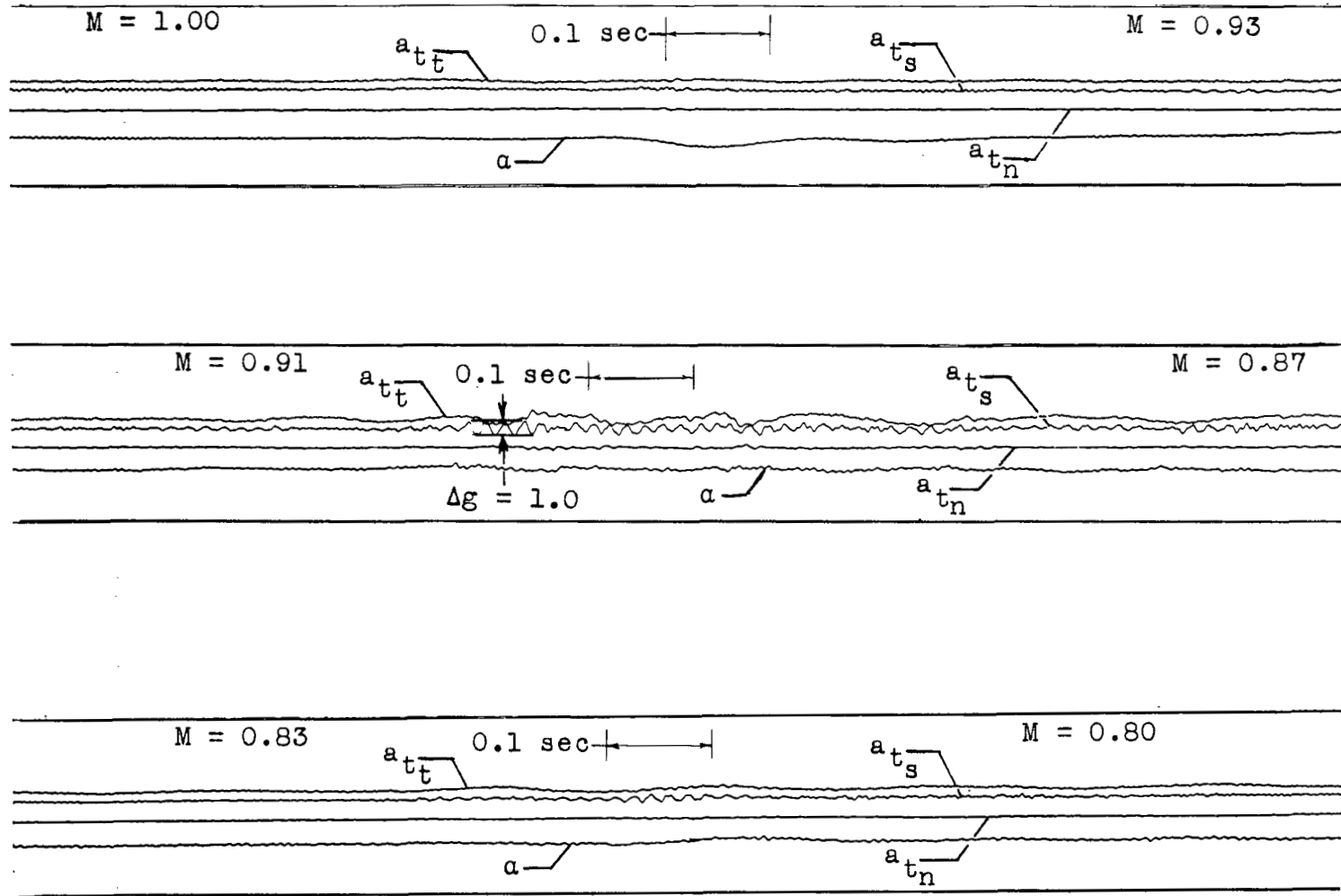


Figure 12.- Variation with Mach number of trim angle of attack, normal-force coefficients, and side-force coefficients.



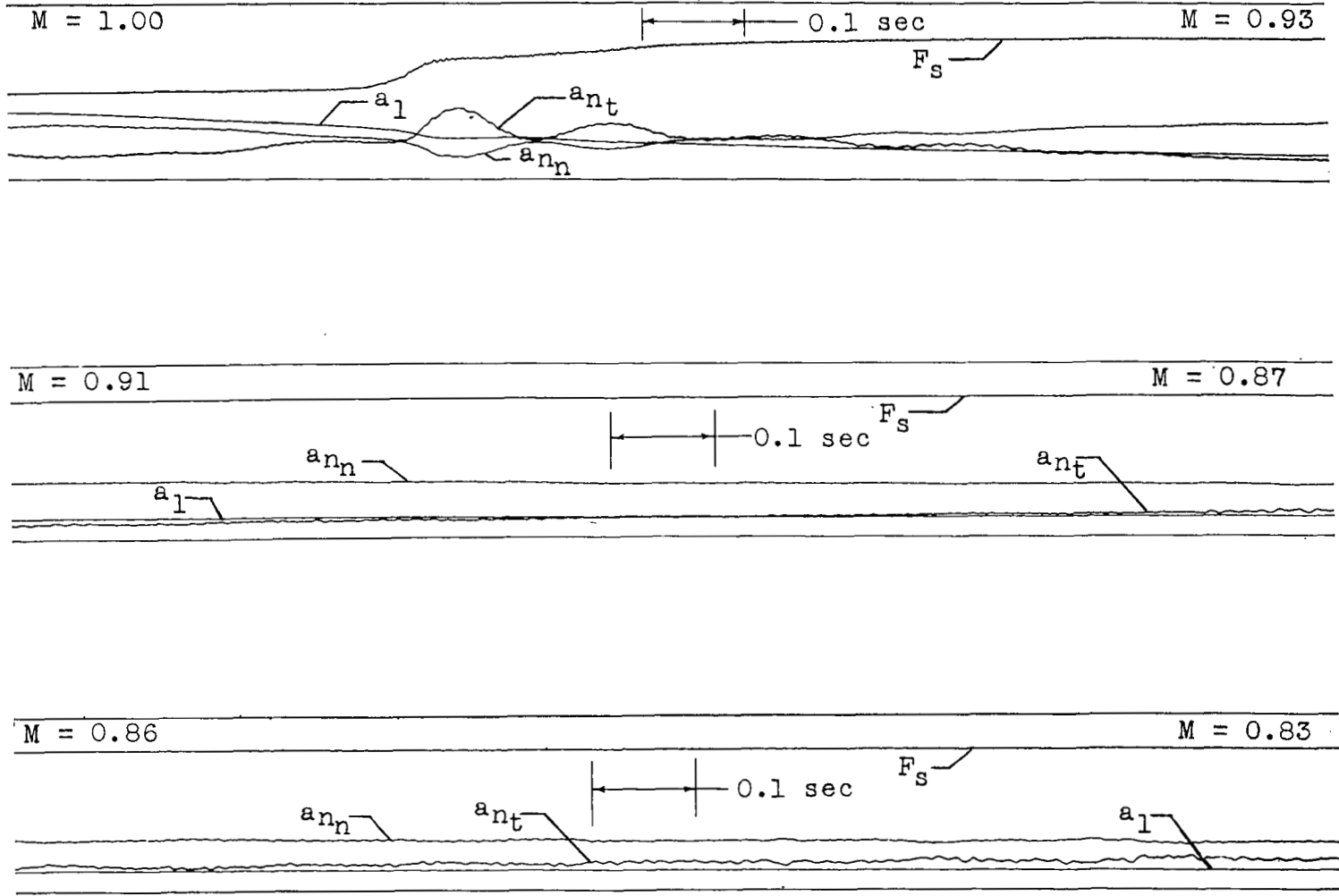
(a) Configuration with tank A.

Figure 13.- Reproduction of portions of teletype records obtained in tests of wing-mounted external stores.



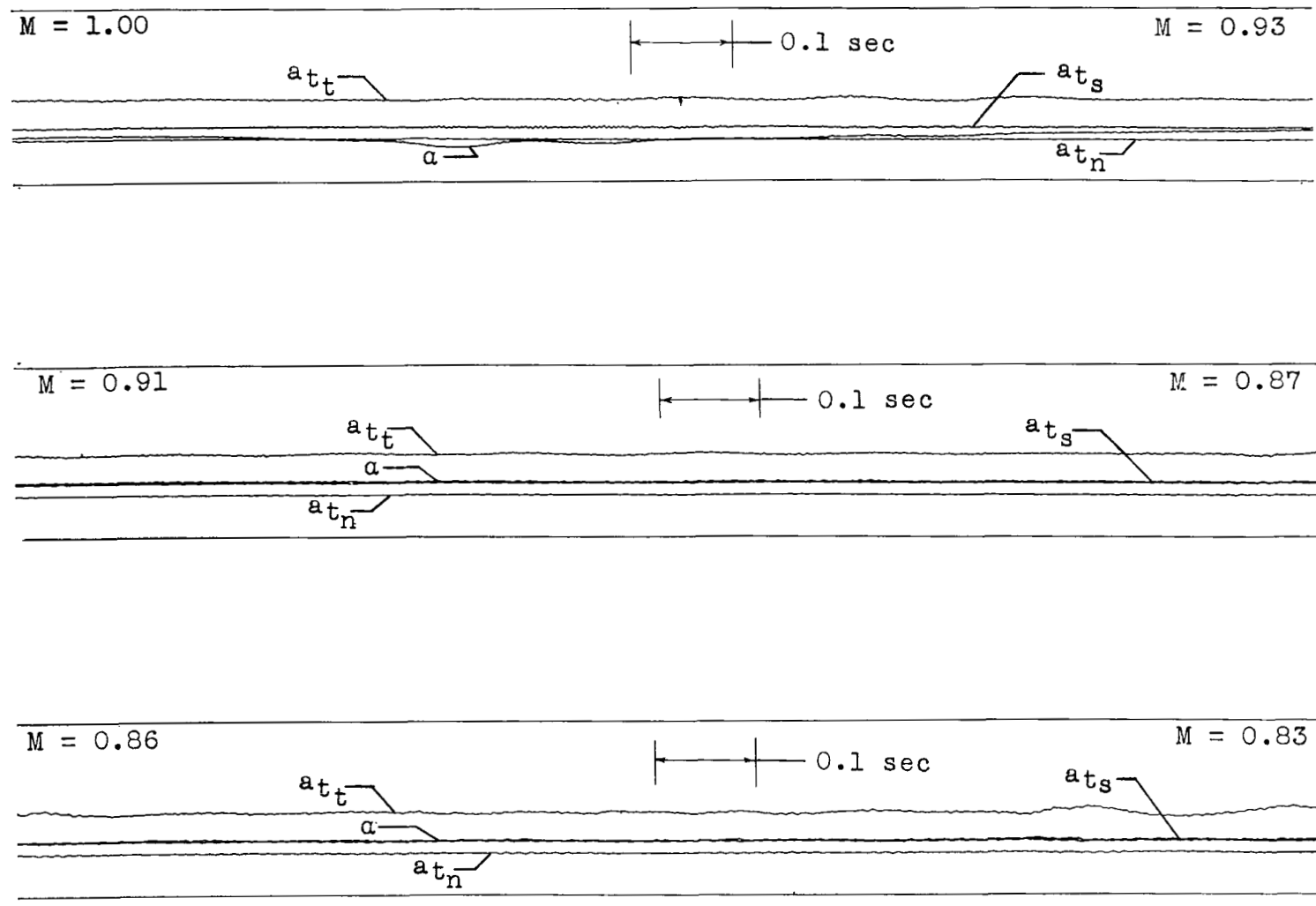
(a) Concluded.

Figure 13.- Continued.



(b) Configuration with tank B.

Figure 13.- Continued.



(b) Concluded.

Figure 13.- Concluded.

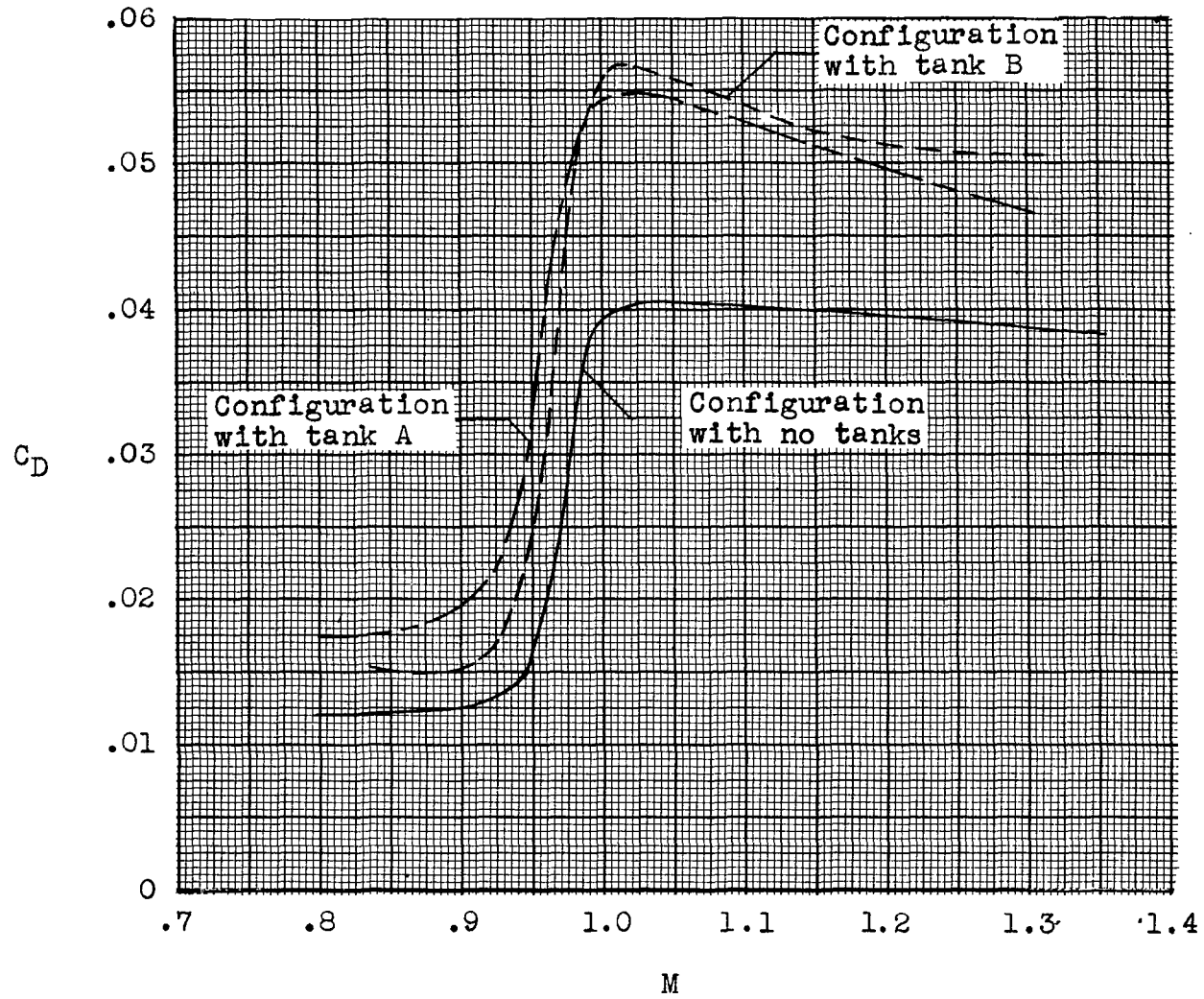
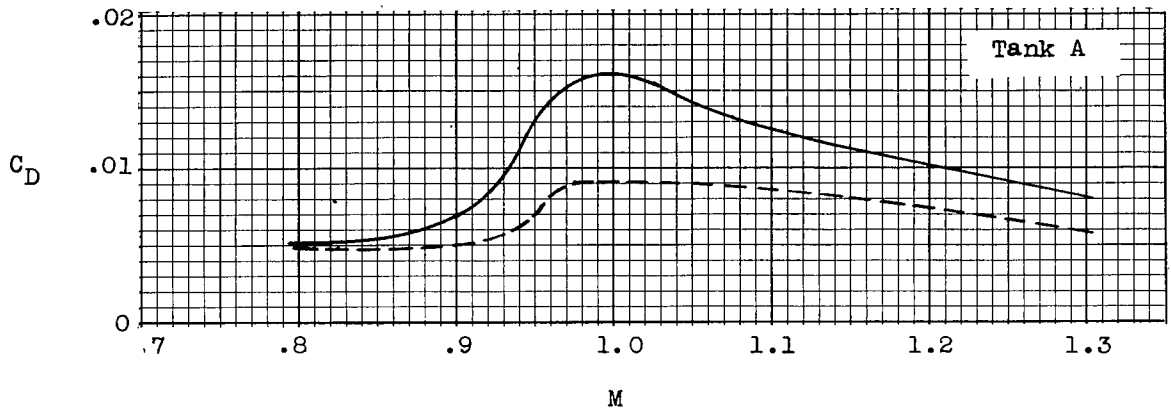


Figure 14.- Variation of total drag coefficient, based on total wing area, with Mach number.



— Total installation drag coefficient of two tanks and pylons
 - - - Twice the drag coefficient of one tank in the presence of the fuselage, wing, and pylon
 - · - Twice the drag coefficient of one isolated tank

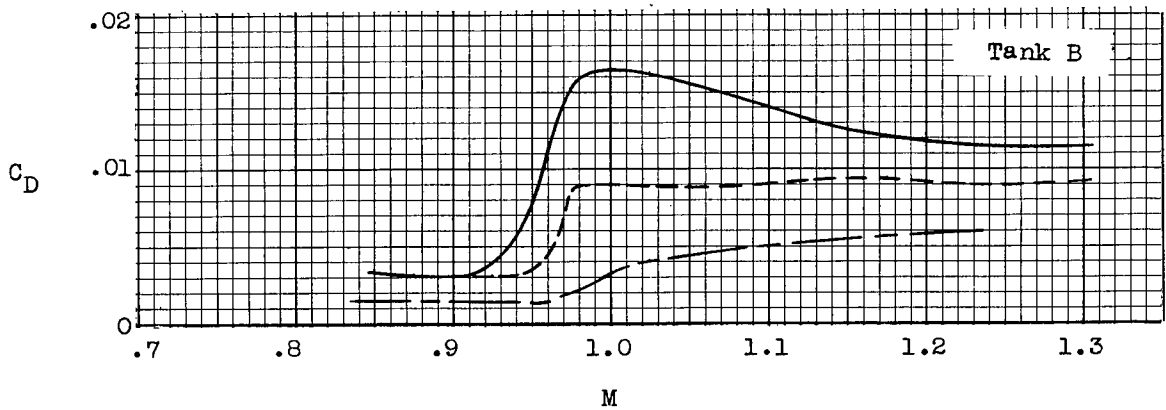


Figure 15.- Variation with Mach number of the increments of drag coefficient caused by pylon mounting two tank-type stores under a sweptback wing.

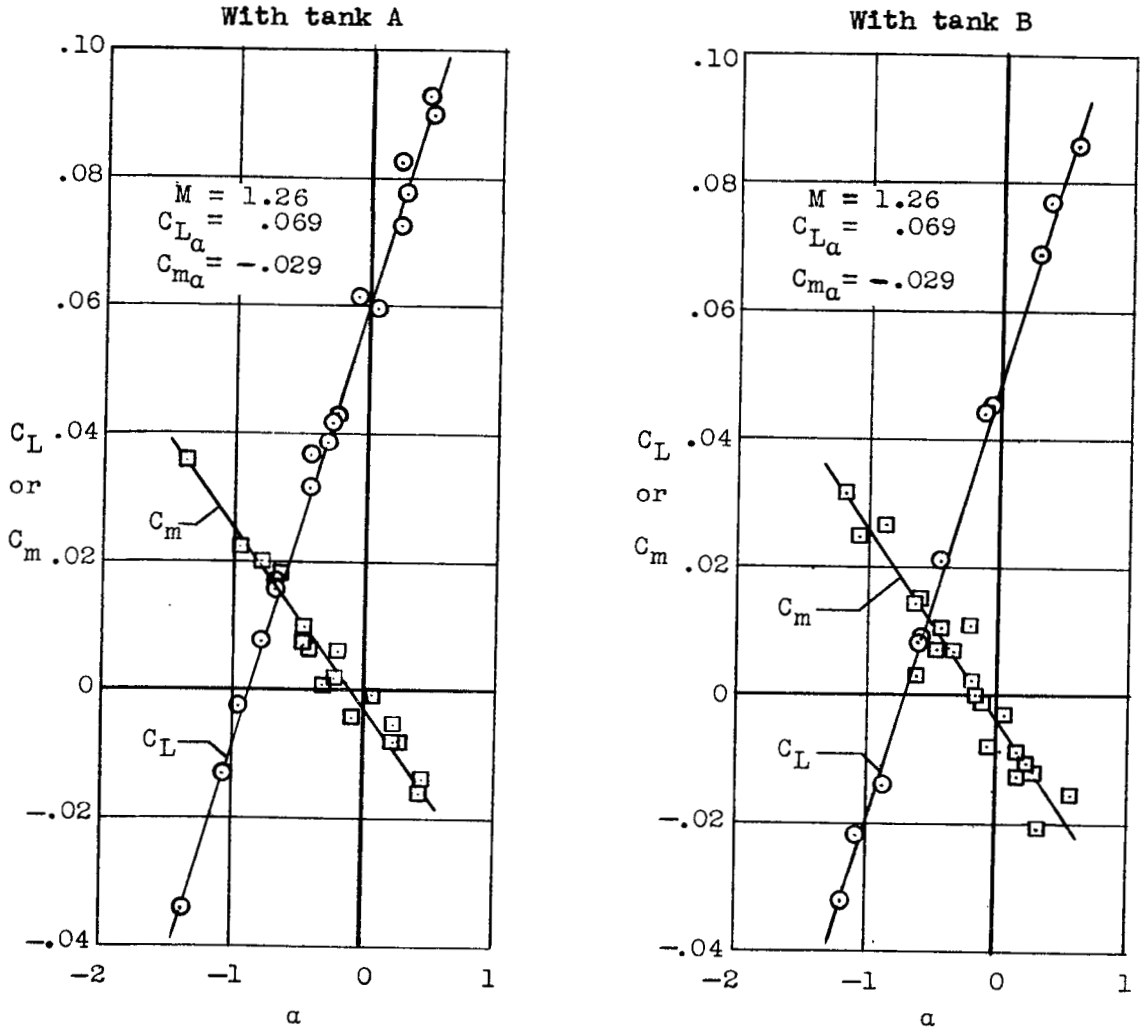


Figure 16.- Variation of lift and pitching-moment coefficients with angle of attack.

NASA Technical Library



3 1176 01437 6934

